Journal of Food Engineering 113 (2012) 442–452

Contents lists available at SciVerse ScienceDirect

Journal of Food Engineering

journal homepage: www.elsevier.com/locate/jfoodeng

Effect of enzymatic treatment on the cross-flow microfiltration of açaí pulp: Analysis of the fouling and recovery of phytochemicals

Rita Margarete Donato Machado *, Renata Natsumi Haneda, Bruno Peruchi Trevisan, Sérgio Rodrigues Fontes

Department of Mechanical Engineering, School of Engineering of São Carlos, EESC, University of São Paulo, USP, Av. Trabalhador São-carlense 400, 13566-590 São Carlos, SP, Brazil

ARTICLE INFO

Article history:
Received 16 February 2012
Received in revised form 28 May 2012
Accepted 30 June 2012
Available online 10 July 2012

Keywords:
Microfiltration
Açaí pulp
Enzymatic treatment
Polyphenols
Antioxidant capacity

ABSTRACT

This study aimed to investigate the effects of pectinase enzyme treatment of açaí pulp on cross-flow microfiltration (CFMF) performance and on phytochemical and functional characteristics of their compounds. Analyses of fouling mechanisms were carried out through resistance in series and blocking in law models.

The enzymatic treatment was conducted using Ultrazym® AFPL (Novozymes A/S) at 500 mg kg^{-1} of açaí pulp for 30 min at 35 °C. Before microfiltrations, untreated and enzyme-treated açaí pulps were previously diluted in distilled water (1:3; w/v).

CFMFs were conducted using commercial α-alumina (α-Al_2O_3) ceramic membranes (Andritz AG, Austria) of 0.2 μm and 0.8 μm pore sizes, and 0.0047 m^2 of filtration area. The microfiltration unit was operated in batch mode for 120 min at 25 °C and the fluid-dynamic conditions were transmembrane pressure of ΔP = 100 kPa and cross-flow velocity of 3 m s^{-1} in turbulent flow.

The highest values of permeate flux and accumulated permeate volume were obtained using enzyme-treated pulp and 0.2 μm pore size membranes with steady flux values exceeding 100 L h^{-1} m^{-2}. For the 0.8 μm pore size membrane, the estimated total resistance after the microfiltration of enzyme-treated açaí pulp was 21% lower than the untreated pulp, and for the 0.2 μm pore size membrane, it was 18%. Cake filtration was the dominant mechanism in the early stages of most of the CFMF processes. After approximately 20 min, however, intermediate pore blocking and complete pore blocking contributed to the overall fouling mechanisms.

The reduction of the antioxidant capacity of the permeates obtained after microfiltration of the enzyme-treated pulp was higher ($p < 0.01$) than that obtained using untreated pulp. For total polyphenols, on the contrary, the permeates obtained after microfiltration of the enzyme-treated pulp showed a lower mean reduction ($p < 0.01$) than those from the untreated pulp. The results show that the enzymatic treatment had a positive effect on the CFMF process of açaí pulp.

1. Introduction

Açaí (*Euterpe oleracea* Mart.) is a palm tree fruit found throughout the Amazon estuary floodplains. Açaí pulp is typically consumed *in natura* or added as an ingredient to various food products and beverages (Rogez, 2000; Menezes et al., 2008). In Brazil, the state of Pará is the main natural dispersion center for the açaí palm, generating approximately 95% of the national production.

Açaí pulp is considered a high-nutrition food due to its large amount of lipids (mostly unsaturated fatty acids), protein, minerals and insoluble dietary fiber (Menezes et al., 2008; Schauss et al., 2006). The fruit has also received international interest due to the potential health benefits associated with its phenolic composition and antioxidant capacity (Pozo-Insfran et al., 2004; Lichtenthäler et al., 2005).

Açaí is rich in anthocyanins, a group of polyphenols included in the flavonoid class, constituting the glycosides of polyhydroxyl and polymethoxyl derivatives of 2-phenylbenzopyrylium (flavylium cation). The two major anthocyanins found in açaí are cyanidin-3-glucoside and cyaniding-3-rutinoside (Pozo-Insfran et al., 2004; Lichtenthäler et al., 2005). Anthocyanins are water-soluble plant pigments responsible for the orange, red and blue colors of fruits, flowers and vegetables (Castañeda-Ovando et al., 2009). These flavonoids have been the subject of numerous studies over their possible use as a source of natural pigments and their high capacity to scavenge free radicals associated with the prevention of cardiovascular and degenerative diseases (Kris-Etherton et al., 2002; Szajdek and Borowska, 2008).

* Corresponding author. Tel.: +55 16 3373 9531; fax: +55 16 3373 9402.
E-mail address: ridonato@hotmail.com (R.M.D. Machado).

0260-8774
http://dx.doi.org/10.1016/j.jfoodeng.2012.06.022

However, the poor stability of anthocyanins is affected by their chemical structure, environmental factors such as pH, temperature, oxygen, light, and by the presence of other phytochemicals in the solution (Pozo-Insfran et al., 2004; Castañeda-Ovando et al., 2009). To minimize the loss of functional properties of products made from açaí, careful studies on the processing and handling practices are necessary. Cross-flow microfiltration (CFMF) using ceramic membranes has been evaluated as an alternative to conventional processes for the clarification of açaí pulp. This technology can be used to stabilize the functional and microbiological characteristics of açaí products by reducing adverse effects associated with thermal treatments. CFMF can also be employed in the integrated membrane processes as a preliminary treatment to recover bioactive compounds from açaí, resulting in a product that can be used as a functional ingredient in the food and beverage industries.

The main drawback to using membrane technology has been the permeate flux decay as a function of operation time due to the high concentration of soluble and insoluble solids in the raw material. Several mechanisms, such as concentration polarization and fouling, are involved in reducing the permeate flux. Concentration polarization is a reversible phenomenon in which the solute or particle concentration in the vicinity of the membrane surface is higher than that in the bulk. Polarized layer or cake layer occurs when hydrocolloids, macromolecules and other relatively larger solutes are filtered and accumulated at the membrane surface, providing additional hydraulic resistance to the permeate flux with time in a microfiltration process (Belfort et al., 1994; Song and Elimelech, 1995; Dufrèche et al., 2002). The rapid permeate flux decline at the start of cross-flow operations has been attributed to the formation of the cake layer at the membrane surface. Changes in operating conditions, such as increasing the feed velocity and/or decreasing the transmembrane pressure or feed concentration, contribute to reduce the thickness of the cake layer and increase the permeate flux (Zeman and Zydney, 1996; Cheryan, 1998). Membrane fouling is characterized by an irreversible pore blockage caused by the deposition and accumulation of feed components on the surface and/or within the membrane pores (by adsorption or physical blockage of pores). The fouling phenomenon occurs due to specific solute–solute and solute–membrane physical and chemical interactions which are independent of changes in operating conditions. In this case, permeate flux recovery is only possible after chemical cleaning of the membrane (Cheryan, 1998).

In general, the greatest resistance to permeate flux during the filtration of fruit juices is provided by cell-wall polysaccharides such as protopectin, cellulose, hemicellulose and lignin in the raw materials. Consequently, pectinolytic enzymes like polygalacturonase, pectin methylesterase and pectin lyase have long been used to increase clarification and reduce viscosity in juices (Vaillant et al., 1999; Yu and Lencki, 2004; Ushikubo et al., 2007; Koponen et al., 2008). Pectinases are a group of enzymes that degrade pectic substances by hydrolyzing glycosidic bonds along the carbon chain (Benen et al., 2003). Concomitant with increasing filtration performance, enzymatic treatment has also been used to enhance the extractability of phenolic components through the degradation of skin cell wall material (Bagger-Jørgensen and Meyer, 2004).

To investigate permeate flux decay and how to minimize it, different membrane pore blocking models have been used to identify the most prominent flux decline mechanisms during the microfiltration process (Hermia, 1982; Field et al., 1995; Arnot et al., 2000; Lim and Bai, 2003; Mirsaeedghazi et al., 2010).

The analysis for predicting flux decline by resistance in series has been a practical approach in modeling complex processes. The membrane is considered a thickness barrier of resistance (R) with intrinsic hydraulic resistance (R_M), which depends on its manufacturing procedure and respective morphology. In the solutes separation process an additional resistance (R_C) is related to the concentration polarization and to the cake layer due to high concentration of solutes at the membrane surface. As the irreversible impregnation (fouling) mechanism is also present during most of the process, one respective extra resistance (R_F) must be added. Assuming that all the resistances – membrane, cake layer and fouling – act in series, the permeate flux can be expressed according to Darcy's law, which considers total resistance to the permeate flux as the sum of all resistances (Cheryan, 1998).

Mathematical modeling of flux decline behavior using empirical models was first proposed by Hermia (1982), based on the membrane separation processes being conducted under constant pressure. Hermia described modes of membrane pore blocking where the fouling mechanisms were represented by four different conditions: cake filtration, standard blocking, incomplete pore blocking and complete blocking. The models originally applied to dead-end filtration were later modified for CFMF (Field et al., 1995; Arnot et al., 2000). Recently, mathematical blocking models have been used to determine the fouling mechanisms involved in CFMF, and have achieved relative success in the modeling of complex fluids (Arnot et al., 2000; Almandoz et al., 2010; Li et al., 2010).

Considering consumer demand for high-quality foods, there is a need to define processing operations which allow açaí pulp to maintain its functional characteristics. Accordingly, this study was designed to investigate the effects of pectinase enzyme treatment of açaí pulp on CFMF performance. Analyses of fouling mechanisms were carried out through resistance in series and blocking in law models. The recovery of phytochemicals via total polyphenols and antioxidant capacity analysis was also examined.

2. Experimental

2.1. Chemicals

Folin & Ciocalteu's phenol reagent, 2,2-diphenyl-1-picrylhydrazyl (DPPH), and the standards 6-hydroxy-2,5,7,8-tetramethylchromane-2-carboxylic acid (trolox) and gallic acid were obtained from Sigma–Aldrich (Sigma–Aldrich Co., St. Louis, USA). HPLC grade absolute ethyl alcohol, anhydrous sodium carbonate and sodium hydroxide were acquired from J.T. Baker (Mallinckrodt Baker, S.A., Mexico).

2.2. Açaí pulp and pre-treatments

Commercial frozen açaí pulps (medium type: 11–14% of total solids) manufactured in the Brazilian city of Belém (Pará state) were acquired in the city of São Carlos (São Paulo state) and stored at −18 °C until microfiltration processing. The frozen pulp used in the experiments was obtained from the same supplier and thawed at temperatures of under 40 °C before conducting the tests.

Enzymatic treatment was carried out using Ultrazym® AFPL (Novozymes A/S – Bagsvaerd, Denmark) at 500 mg kg^{-1} of açaí pulp for 30 min at 35 °C. Concentration and reaction temperature were chosen based on the previous assays that evaluated the apparent viscosity reduction of the açaí pulp treated with Ultrazym® AFPL. To evaluate the enzymatic treatment effects, samples were withdrawn at 0, 30, 90 and 120 min intervals of incubation for rheological measurements using a rotational rheometer DVIII+ (Brookfield Engineering Laboratory, Massachusetts, USA), equipped with stainless steel cone-plate at 25 °C.

Before CFMF, samples of untreated and enzyme-treated açaí pulp were previously diluted in distilled water (1:3; w/v) and fitted using a stainless steel sieve with a 0.50 mm wire diameter.

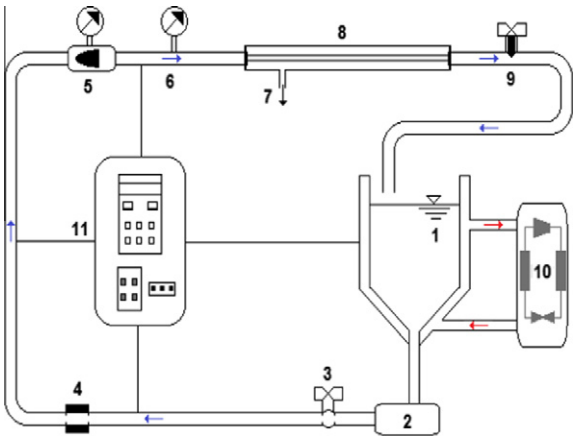

Fig. 1. Microfiltration test bench unit. (1) Double wall feeding tank; (2) positive displacement pump; (3) bleeder valve; (4) pressure switch; (5) flow meter; (6) pressure gauge; (7) permeate exit; (8) module for tubular ceramic membrane installation; (9) flow control valve; (10) refrigeration circuit; (11) electronic control unit for the elements: 2, 4, 5 and 10.

2.3. MF experimental setup

Cross-flow microfiltrations were conducted using commercial α-alumina (α-Al_2O_3) ceramic membranes (Andritz AG, Austria) with pore sizes of 0.2 μm and 0.8 μm, single-channel tube of 0.006 m inner diameter, 0.25 m in length and 0.0047 m^2 of filtration area. A bench-top test unit was used in the CFMF experiments (Fig. 1). The system was built using AISI 304 stainless steel and included a double wall feeding tank (10 L), positive displacement pump (NETZSCH Ltd., Brazil) for the flow, bleed valve to improve circuit cleaning, pressure switch, flow meter, pressure gauge, module for the ceramic tubular membrane installation, flow control valve, refrigeration system and an electronic control unit. The positive displacement pump was regulated by a frequency converter to ensure constant transmembrane pressure, which was manually controlled throughout the assays.

The temperature of the açaí suspension in the feed tank was controlled at 25 ± 1 °C during the microfiltration processes using a thermocouple device linked to a refrigeration system, and a centrifugal pump to circulate cold water inside the double wall of the feed tank. The microfiltration unit was operated in batch mode for 120 min. A summary of the fluid-dynamic conditions is given in Table 1.

Table 1
Processing parameters of the microfiltration experiments, which were performed in the sequence below.

Experiments	Processing parameters				C_F[c]
	Membrane pore size (μm)	Enzymatic treatment of the açaí pulp[a]	Transmembrane pressure (kPa)	Cross-flow velocity ($m\ s^{-1}$)	
MF1	0.8 (A)[b]	Without	100	3.2	1.10
MF2	0.8 (A)	With	100	3.2	1.13
MF3	0.2 (B)	Without	100	3.2	1.18
MF4	0.2 (B)	With	100	3.2	1.22
MF5	0.2 (C)	With	100	3.2	1.25
MF6	0.2 (C)	Without	100	3.2	1.18

[a] Enzymatic treatment of açaí pulp using Ultrazym® AFPL at 500 mg kg^{-1} for 30 min at 35 °C.
[b] A, B and C refer to different alumina ceramic membranes used in the microfiltrations.
[c] CF – concentration factor was calculated by dividing the weight of the feed (kg) by the weight of the retentate (kg).

To evaluate the enzymatic treatment effects, at every 5 min the permeate was collected and weighed on an electronic scale (BEL Engineering, Monza, Italy) to obtain the permeate flux (J, $L\ h^{-1}\ m^{-2}$) behavior during the microfiltrations. J was calculated using the following equation:

$$J = \frac{m}{tA\rho} \tag{1}$$

where m is the permeate mass collected during the microfiltration (kg), t is the filtration time (h), A is the effective filtration area (m^2), and ρ is the permeate density ($kg\ m^{-3}$).

The retentate was recycled in the feed tank, while the permeate was collected during the microfiltration process for further analysis. Collected samples of açaí pulp, feed suspension, permeate and retentate were frozen and stored at −18 °C until total polyphenols and antioxidant capacity analysis.

2.4. Cleaning procedure

At the end of the microfiltration processes, the system (bench-top test unit and membrane) was rinsed with distilled water to remove the cake layer deposited on the membrane surface, and the water flux was measured under similar operating conditions. This was followed by a chemical cleaning carried out in two stages. First, 0.5% alkaline detergent Extran® MA 01 (Merck KGaA, Darmstadt, Germany) was heated to 50 °C and circulated in the system for 20 min under cross-flow velocity of 3 $m\ s^{-1}$ – 10 min without transmembrane pressure ($\Delta P = 0$ kPa) and 10 min with $\Delta P =$ 100 kPa. The system was then rinsed with distilled water to completely remove the detergent solution.

The membrane was then removed from the microfiltration test unit and left in 1% enzymatic detergent MIX UF10 (Mixing Quimica Ind. e Comércio, Brazil) at room temperature (approximately 25 °C) for about 12 h, after which the membrane was rinsed with distilled water and returned to the microfiltration test unit. The second stage of the chemical cleaning was similar to the first, except for the addition of 200 ppm of sodium hypochlorite (NaClO) to the 0.5% alkaline detergent solution. After being rinsed with distilled water, the membrane was dried in an oven for 1 h at 70 °C.

The effectiveness of the membrane cleaning was evaluated through flux recovery (FR, %), whereby the water flux after chemical cleaning (J_{wc}) was compared with the initial water flux by using a new membrane (J_w) (Astudillo et al., 2010). Both were measured under similar operating conditions and FR was calculated using the following expression:

$$FR = \left(\frac{J_{wc}}{J_w}\right)100 \tag{2}$$

2.5. Analysis of the permeate flux decay

2.5.1. Resistance in series model

According to Darcy's law the permeate flux is expressed as:

$$J = \frac{\Delta P}{\mu(R_T)} \tag{3}$$

where J is the permeate flux ($m^3\ s^{-1}\ m^{-2}$), ΔP is transmembrane pressure (kPa) and μ is cinematic fluid viscosity (Pa s) (Cheryan, 1998).

Total membrane resistance (R_T), which is the sum of the resistances to flow, was calculated using Eq. 3, in which R_T was estimated using the average permeate flux (J) measured 20 min after the beginning of each microfiltration, when the cake layer was considered settled.

According to the resistance in series model, R_T can be expressed as:

$$R_T = R_M + R_F + R_C \quad (4)$$

where R_M is membrane resistance (m^{-1}); R_F is resistance related to fouling (m^{-1}), and R_C is resistance related to cake layer (m^{-1}). The resistance related to concentration polarization was considered not significant (zero).

Intrinsic hydraulic resistance of the membrane was calculated using the measurements taken from the initial water flux (J_w) using the new membranes. Resistance related to fouling was estimated using water flux measurements taken after rinsing the membrane, subsequent to the microfiltration runs. Resistance related to cake layer was estimated using Eq. 4.

2.5.2. Blocking in law model

The membrane fouling mechanisms responsible for reduced flux behavior were also analyzed using empirical models proposed by Hermia (1982), originally applied to dead-end filtration conducted under constant pressure (Eq. 5) and then modified for use in the cross-flow filtration analysis (Eq. 6) by Field et al. (1995).

$$\frac{d^2t}{dV^2} = k\left(\frac{dt}{dV}\right)^n \quad (5)$$

$$\frac{-dJ}{dt}J^{n-2} = k(J - J^*) \quad (6)$$

where k and n are the phenomenological coefficient and general index of modeling, respectively, J_0 is the initial permeate flux of the process, and J^* represents the steady-state flux.

In the case of this study, we point out that because of the reduced permeation area, the concentration rate was low (CF ranged from 1.10 to 1.25) (Table 1); barely interfering in the properties of the fluid. Thus, according to the graphically presented results, it was assumed that the permeate flux value (J_f) at the end of the microfiltration (120 min) was in a "pseudo steady-state" condition.

In the general equation, which is characteristic of CFMF, the coefficient k and index n can take different values, depending on the fouling mechanism (Field et al., 1995).

To identify the main cause of the flux decay during CFMF of açaí pulp, four fundamental fouling mechanisms derived from Eq. 6 were examined as follows:

2.5.2.1. Cake filtration (n = 0). Relatively large solutes such as hydrocolloids and macromolecules are rejected by the membrane, i.e., they do not enter the pores, and form a layer at the membrane surface. In this case the cake and membrane resistances comprise overall resistance.

$$k_0 t = \frac{1}{J_f^2}\left[\ln\left(\frac{J}{J_0}\cdot\frac{J_0 - J_f}{J - J_f}\right) - J_f\left(\frac{1}{J} - \frac{1}{J_0}\right)\right] \quad (7)$$

2.5.2.2. Intermediate pore blocking (n = 1.0). Where the particles block only a fraction of the pores, and the particles accumulated on the membrane surface are also taken into account.

$$k_{1.0}t = \frac{1}{J_f}\left[\ln\left(\frac{J_0 - J_f}{J_0}\cdot\frac{J}{J - J_f}\right)\right] \quad (8)$$

2.5.2.3. Standard pore blocking (n = 1.5). Also known as internal pore blocking, this mechanism occurs when the pore volume decreases due to the deposition or adsorption of microsolutes and/or macromolecules within the pores.

$$\frac{1}{J^{0.5}} = \frac{1}{J_0^{0.5}} + k_{1.5}t \quad (9)$$

2.5.2.4. Complete pore blocking (n = 2.0). When each particle reaching the membrane surface contributes to blocking the pores and completely sealing the filtration area.

$$J = (J_0 - J_f)\exp(-k_{2.0}J_0 t) + J_f \quad (10)$$

The k parameter estimate was performed through a non-linear regression optimization procedure using the STATISTICA® program. For each set of $J \times t$ experimental data, a series of four optimization runs were sequentially performed, where n was equal to 0, 1.0, 1.5, and 2.0. The corresponding initial flux (J_0) and terminal flux (J_f) values were obtained from the experiments.

The dominant fouling mechanism was established by comparing the correlation coefficients between numerical predictions and experimental data.

2.6. Phytochemical characterization

Total phenolic content in the samples was determined using the Folin–Ciocalteu colorimetric method (Singleton and Rossi, 1965) optimized by George et al. (2005). Prior to the analysis, the samples were diluted in distilled water (1:100 for pulp and 1:20 for feed suspension, permeate and retentate) to obtain absorbance readings at 760 nm within a 0.1–0.7 range. Calibration curve linearity was obtained using the gallic acid standard in the 10–75 mg L^{-1} concentration range. Total polyphenols were expressed as gallic acid equivalents (GAE) (mg of gallic acid) per 100 mL of sample.

Antioxidant capacity was measured in terms of the free radical scavenging activity of the açaí samples, following the DPPH· (free radical 2,2-diphenyl-1-picrylhydrazyl) assay based on Brand-Williams et al. (1995) with modifications. Aliquots of 0.1 mL of açaí samples diluted in distilled water, as mentioned above, were added to 3.9 mL of a 0.05 mmol L^{-1} solution of DPPH· in ethanol. The mixtures were incubated in the dark at room temperature, and after 15 min of reaction, the absorbance was read at 517 nm in a spectrophotometer (Biospectro SP-22). Trolox was used as the reference antioxidant compound in the 0–1000 μmol L^{-1} concentration range. The results were expressed as μmol of trolox equivalent antioxidant capacity (TEAC) per 100 mL of sample. All determinations were made in triplicate.

The effect of the enzyme treatment on the reduction (R%) of total polyphenols and antioxidant capacity, after the membrane microfiltration process, was evaluated as follows:

$$R = 1 - \left(\frac{C_p}{C_F}\right)100 \quad (11)$$

where C_P represents the concentration of the solute at the permeate, and C_F is the concentration at the feed.

Data analysis was performed by determining the mean of three values, and calculating the standard deviations. Polyphenols concentration and capacity antioxidant data were further analyzed using a t-test (Miller and Miller, 1993).

3. Results and discussion

3.1. Permeate flux behavior

Fig. 2(a) shows a typical flux behavior for filtration of diluted açaí pulp using alumina ceramic membranes. At the beginning of the microfiltration process the permeate flux was high, particularly when the pulp was treated with Ultrazym® AFPL. However, after 20 min of the process the flux behavior was more constant, with a slight decay.

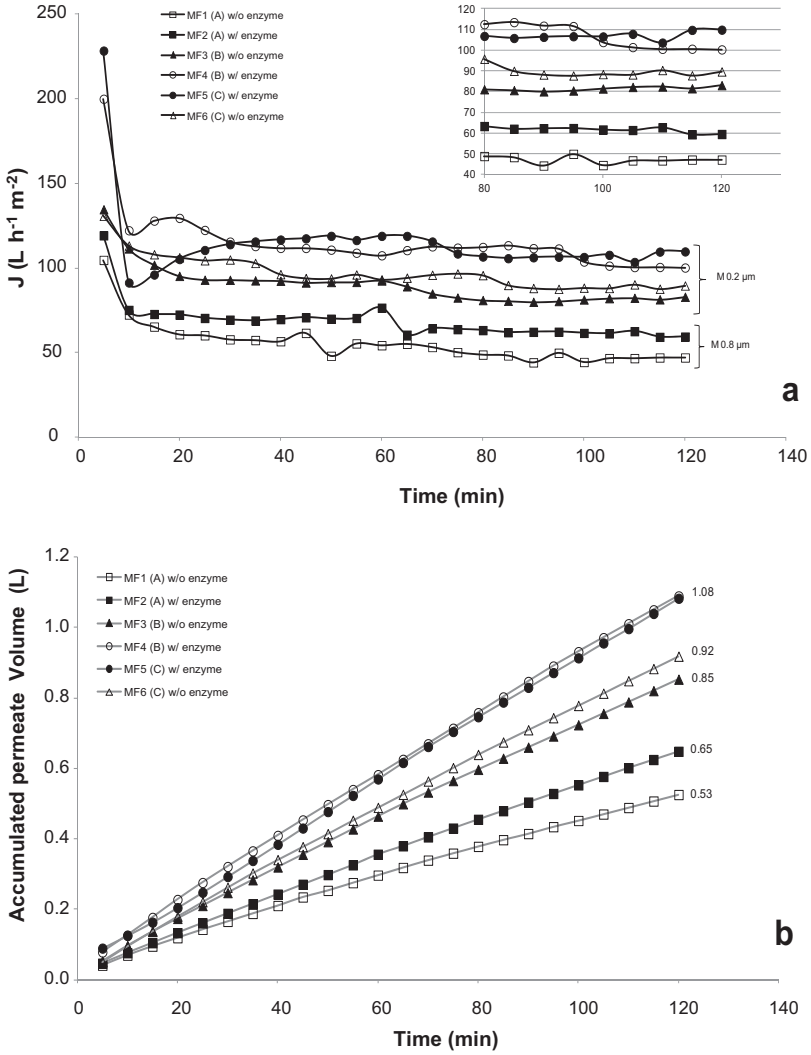

Fig. 2. Cross-flow microfiltrations experiments of diluted açaí pulp (treated or untreated with Ultrazym® AFPL) using 0.2 μm and 0.8 μm pore size ceramic membranes. The fluid-dynamics conditions consisted of transmembrane pressure of ΔP = 100 kPa and cross-flow velocity of 3 m s^{-1} in turbulent flow (Re = 21,000). A, B and C refer to different membranes. (a) Permeate flux (J) vs. filtration time (min); (b) Accumulated permeate volume vs. filtration time (min).

This rapid permeate flux decline at the start of cross-flow operations has been attributed to the formation of a cake layer at the membrane surface. Açaí fruit is rich in lipids (5–7% on a wet basis), protein and insoluble dietary fiber (Menezes et al., 2008; Schauss et al., 2006), and deposition of these compounds on the membrane surface during the first minutes of the microfiltration contribute to the formation of this layer.

The highest values of permeate flux and accumulated permeate volume (Fig. 2a and b) were obtained using 0.2 μm pore size membranes with steady flux values higher than 83 L h^{-1} m^{-2}, indicating good performance for membrane application.

The lowest performance of the 0.8 μm pore size membrane may be correlated with the particle size in the feed solution. A study (Trevisan, 2011) conducted in our laboratory, using acoustic attenuation spectroscopy (APS-100 – Matec Applied Science, Northborough, USA) for particle size analysis of five commercial brands of açaí pulp, found that most particles had a diameter less than 0.6 μm. As a consequence, small particles less than 0.8 μm in diameter could pass through the cake layer and plug the pores via adsorption or physical blockage, thereby increasing resistance to the flow. For the 0.2 μm pore size membrane, results indicate that obstruction of the pores caused by adsorption or physical blockage should have occurred with less intensity due to the considerable presence of particles of more than 0.2 μm in diameter.

Evaluation of the enzyme treatment effect on the performance of the microfiltration membrane was made by comparing experiments conducted with the same membrane. The CFMF using enzyme-treated pulp resulted in the highest permeate flux and accumulated permeate volume values. Açaí fruits are rich in dietary fiber, which consists primarily of pectic substances, cellulose and hemicelluloses. These compounds negatively affect the microfiltration membrane clarification process due to their fibrous nature, and their amounts can vary widely, from 44% to 71% of dry weight. A 3% average that comprises pectins (Schauss et al., 2006; Borovik, 2010; Rufino et al., 2011).

Pectinases act on the destabilization of the pectin–protein complex, which is formed by positively charged proteins covered by a layer of pectin. The hydrolysis of the protective pectin coating exposes positive charges that can initiate aggregation, leading to increased particle size and decreased viscosity (Pilnik and Voragen, 1993; Kashyap et al., 2001; Yu and Lencki, 2004), which improved the performance of the membranes when the enzyme-treated pulp was microfiltered.

The commercial enzyme preparation Ultrazym® AFPL used in this study is characterized by prevailing pectin lyase (PL) activity which acts on the pectic substances. PLs are of particular interest in the processing of fruit juices due to the direct degradation of pectin polymers by the β-elimination mechanism, resulting in

Table 2
Evaluation of cleaning effectiveness through percentage flux recovery (FR) using water flux data of new, fouled (after rinsing with water to remove cake layer) and cleaned membranes.

Experiments	New (J_w) ($L\,h^{-1}\,m^{-2}$)	Fouled ($L\,h^{-1}\,m^{-2}$)	After chemical cleaning (J_{wc}) ($L\,h^{-1}\,m^{-2}$)	FR (%)
MF1	11906	75	9243	78
MF2	11906	219	9940	83
MF3	4458	236	4103	92
MF4	4458	269	4068	91
MF5	7514	236	6428	86
MF6	7514	391	6698	89

the formation of 4,5-unsaturated oligogalacturonides, while other pectinases act sequentially to degrade pectin molecules completely. This leads to a reduction in the viscosity of the juices without negatively affecting the ester groups responsible for specific aromas of various fruits (Benen et al., 2003; Yadav et al., 2009).

3.2. Membrane chemical cleaning effectiveness

Before microfiltrations MF1, MF3 and MF5 of açaí pulp (Table 1), initial water fluxes were measured by passing distilled water through the new membranes, under similar operating conditions, to find the intrinsic membrane resistance (R_M) and initial permeate flux (J_w) of the respective membranes.

Table 2 shows the J_w, J_{wc} and FR values for all microfiltration experiments carried out in this study.

The literature recommends FR values higher than 85% after sequential microfiltrations (Gan et al., 1999; Astudillo et al., 2010). However, in this study the chemical cleaning performed after microfiltrations MF1 and MF2 was unable to restore the water flux to the recommended value, and no additional chemical cleaning was performed to increase FR.

The lowest FR values obtained after chemical cleaning of the 0.8 μm pore size membrane may be related to the particle size in the açaí pulp, and the specific physical and chemical interactions in which these particles are involved, forming a fouling whose removal was more difficult.

3.3. Analysis of the permeate flux decay

3.3.1. Resistance in series model

For the 0.8 μm pore size membrane (membrane A), the estimated total resistance after microfiltration of enzyme-treated açaí pulp ($61.74 \times 10^{11}\ m^{-1}$) was 21% lower than untreated pulp ($78.38 \times 10^{11}\ m^{-1}$). Between MF1 and MF2 a probably irreversible fouling remained, which chemical cleaning did not eliminate. However, this residual resistance was about 0.1% ($0.63 \times 10^{11}\ m^{-1}$) of the estimated R_T for MF2. Resistance values due to fouling and cake layer differed markedly, indicating the nature of the resistance was changed with the enzyme treatment (Fig. 3). The resistance rate related to fouling (69% in MF1), dropped to 27% in MF2.

As mentioned earlier, the diameter of most particles in commercial açaí pulp was less than 0.6 μm, which could contribute to the internal membrane obstruction reducing the permeate flux in MF1. The enzymatic hydrolysis of pectic substances may have caused the destabilization of complex pectin–protein, increasing the particle size and probably affecting the resistance rate due to fouling in MF2.

The R_T values for the microfiltrations using 0.2 μm pore size membranes (membranes B and C) ranged from 36.35×10^{11} to $46.74 \times 10^{11}\ m^{-1}$, while the microfiltrations using enzyme-treated açaí pulp resulted in the lowest R_T values: 22% lower for MF4 than MF3, and 15% lower for MF5 than MF6. The residual fouling resistance rate after cleaning in MF4 and MF6 was less than 2% of the estimated R_T, and did not influence the performance of the membranes.

For the 0.2 μm pore size membrane, resistance values due to fouling and cake layer also differed between microfiltrations of enzyme-treated and untreated pulp, though to a lesser degree (Fig. 3). Resistance due to fouling was 53% of R_T in MF3 and 57% in MF4, indicating a slight increase for enzyme-treated pulp. For microfiltrations using membrane C, resistance due to fouling was 16% in MF5 and 22% in MF6, indicating that enzyme treatment improved permeation, but did not significantly affect the type of resistance. The highest resistance for membrane C was due to cake layer, which was not the case with membrane B, indicating that membranes from the same supplier and with the same pore size can perform differently with respect to resistance type.

The results of this study are consistent with the literature findings for decreased resistance due to enzyme-induced aggregation and its positive effect on the permeate flux (Yu and Lencki, 2004). An enzyme treatment in the microfiltration of umbu juice, using a polymeric membrane, had a positive influence on the clarification process, while most resistances were due to fouling, followed by cake layer (Ushikubo et al., 2007). In a study conducted by Araújo et al. (2011), the enzymatic pretreatment of raw

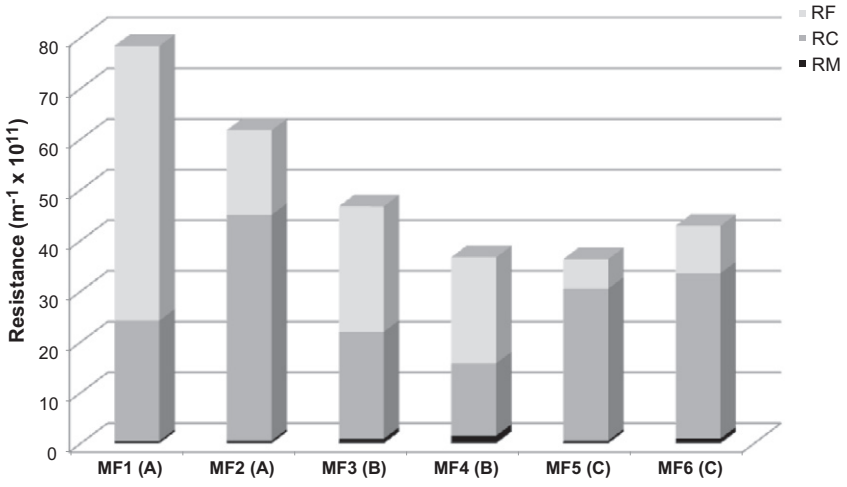

Fig. 3. Effect of enzymatic treatment of açaí pulp on resistance values, calculated according to Darcy's law, where R_C is resistance due to cake layer, R_F is resistance due to fouling, and R_M is membrane resistance.

Table 3
Summary of non-linear regression optimization results (k parameter values) and correlation coefficients (r) between numerical predictions and experimental data for the four fundamental membrane fouling mechanisms.

Experiments	Cake filtration		Intermediate pore blocking		Standard pore blocking		Complete pore blocking	
	K_0	r	$K_{1.0}$	r	$K_{1.5}$	r	$K_{2.0}$	r
MF1	0.001368	0.9539	0.041351	0.9356	0.038335	0.8348	3.247212	0.9169
MF2	0.000884	0.9156	0.038445	0.8517	0.028898	0.7211	3.739404	0.8315
MF3	0.000463	0.9562	0.027716	0.9492	0.018212	0.8428	3.079286	0.9383
MF4	0.000359	0.9393	0.023560	0.8725	0.022162	0.7060	3.816726	0.8593
MF5	0.000289	0.7647	0.052063	0.7660	0.027847	0.3856	9.040855	0.7547
MF6	0.000388	0.9401	0.021356	0.9578	0.013005	0.8811	2.382881	0.9532

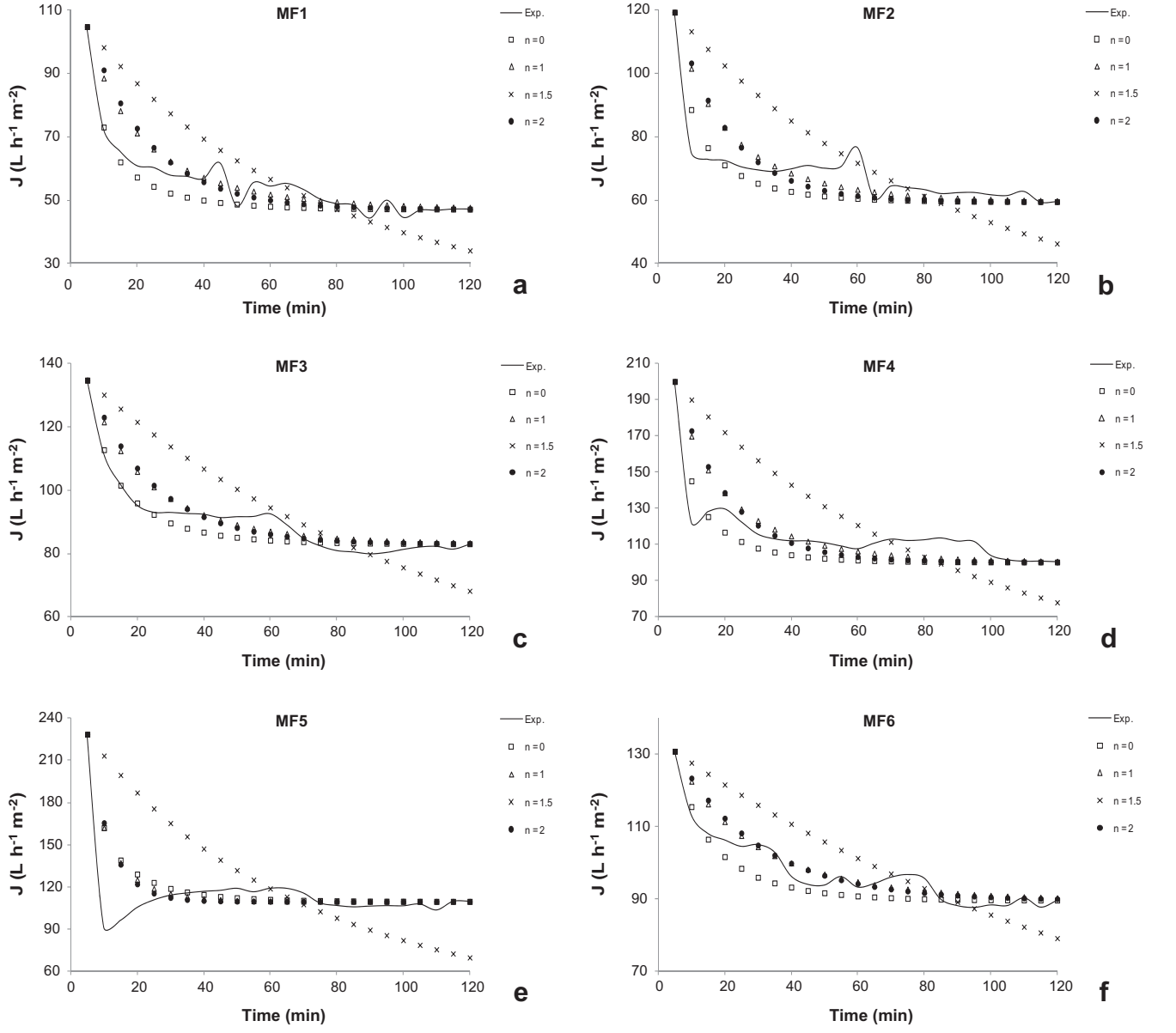

Fig. 4. Flux decay and fouling mechanisms for microfiltrations of enzyme-treated or untreated açaí pulp, where $n = 0$ for cake filtration, $n = 1$ for intermediate pore blocking, $n = 1.5$ for standard pore blocking, and $n = 2$ for complete pore blocking.

blackberry juice using Rapidase® TF (DSM Food Specialities) led to a significant reduction in juice viscosity and had a positive effect on the permeate flux, which maintained a high value throughout the microfiltration process. The authors also found the enzyme treatment was effective in the hydrolysis of macromolecules responsible for fouling.

3.3.2. Blocking in law model

The k parameter values were estimated through non-linear regression optimization, and the correlation coefficients (r) are summarized in Table 3. Comparisons between numerical predictions and experimental data of the microfiltrations assays are shown in Fig. 4.

Table 4
Total polyphenols concentrations in açaí pulp, feed suspension (untreated and enzyme-treated), and products (permeate and retentate) obtained after cross-flow microfiltrations.

Analysis	Samples	Microfiltrations					
		MF1	MF2	MF3	MF4	MF5	MF6
Total polyphenols (mg GAE 100 mL^{-1})	Açaí pulp[a]	513 ± 0.6	510 ± 6.1	585 ± 15.2	542 ± 3.6	563 ± 10.9	525 ± 3.6
	Feed	128 ± 1.0	131 ± 2.9	145 ± 0.2	114 ± 2.6	158 ± 0.9	125 ± 2.8
	Permeate	76 ± 0.8 (41)[b]	83 ± 0.4 (37)	71 ± 0.5 (51)	73 ± 0.4 (36)	84 ± 0.9 (47)	68 ± 0.5 (46)
	Retentate	123 ± 1.3 (4)	109 ± 0.5 (17)	145 ± 6.6 (0)	115 ± 3.1 (0)	138 ± 5.2 (13)	112 ± 0.4 (10)

GAE: gallic acid equivalent per 100 mL of sample.
Data are expressed as the mean of three replicates ± standard deviations.
[a] açaí pulp *in natura* (untreated).
[b] Percentage reduction in comparison with the feed.

The fouling mechanism was identified by using linear regression to estimate the correlation coefficients. Based on "*r*" values the dominant phenomenon for most of the microfiltrations was cake filtration. For MF5 and MF6, however, intermediate pore blocking and complete pore blocking mechanisms also fitted the experimental data well.

With the exception of MF5, for microfiltrations using enzyme-treated pulp, the correlation coefficients for cake filtration were higher than 0.91, while for the other fouling mechanisms the *r* values were lower than 0.86. These findings indicate that cake filtration was the dominant fouling mechanism, probably due to the aggregation of particles induced by enzyme activity, where the macromolecules created were rejected and then accumulated on the membrane surface, forming a cake layer.

Fig. 4(a–f) shows that cake filtration fitted the experimental data well for the first 20–30 min of the microfiltration tests. Subsequently, with the exception of standard pore blocking (which did not fit any experimental data well), all other fouling mechanisms contributed to the fouling process.

The resistance in series model demonstrated that the nature of the fouling (reversible or irreversible) also depended on the membrane used in the microfiltrations. This model is unable to distinguish the moment at which the resistances occur, but can quantify them experimentally, which the pore blocking model did not allow.

A comparison of the two permeate flux decay models showed an agreement in the results when enzyme-treated pulp was used in the MF experiments, specifically a predominance for the formation of a cake layer at the membrane surface.

In recent studies the blocking model has been applied, with relative success, to the cross-flow mode for modeling complex processes. Almandoz et al. (2010) studied the concentration process for dairy proteins using cross-flow ultrafiltration. To determine filtration resistance the authors developed a model for two permeation flux periods. Pore blocking (or incomplete pore blocking) was dominant in the first period, while cake filtration was dominant in the second. Rai et al. (2010) used a blocking model to study flux decline behavior in the microfiltration of watermelon juice, and found cake filtration to be the best flux decline mechanism. Li et al. (2010) analyzed fouling mechanisms by employing a modified model fitted to a non-linear regression procedure, and performed an experimental analysis with scanning electron microscopy. The authors observed that the cake filtration mechanism was dominant in most operating conditions. Hu and Scott (2008) also verified that cake filtration gave the best correlation between model and experimental data in the analysis of the flux decay during cross-flow microfiltration of water in oil emulsions. Moreover, the authors observed that two stages of filtration seemed to occur: the more significant flux decay that occurred in the initial stages of filtration was due to the cake filtration, followed by pore blocking and intermediate pore blocking.

3.4. Phytochemical characterization

Table 4 shows the total polyphenols contents of the açaí pulp, diluted açaí pulp, permeate and retentate samples from the microfiltration experiments.

Total polyphenols concentrations in the açaí pulp samples used in this study ranged from 510 to 585 mg GAE 100 mL^{-1}. Data in the literature concerning content and profile of polyphenols in açaí fruit are scarce and difficult to compare due to the different values achieved. Cruz et al. (2011) found 343.7 ± 15.4 mg GAE 100 g^{-1} of fresh weight (FW), while the phenolic content measured by Pacheco-Palencia et al. (2007) in açaí pulp was 197.2 ± 6.9 mg GAE 100 mL^{-1} of sample. Hassimotto et al. (2005) found 328 ± 0.9 GAE 100 g^{-1} of FW in commercially available frozen açaí pulp. The difference in total polyphenol contents among the various studies that analyzed açaí pulp may have been influenced by factors that include degree of ripeness, variety, processing, storage, and differences in methods used to analyze these compounds.

The polyphenols levels found in açaí pulp (>500 mg GAE 100 mL^{-1} of sample) were higher than those of other Brazilian exotic fruits with considerable market potential, such as murici (159.9 ± 5.6 mg GAE 100 g^{-1} of FW), mangaba (98.8 ± 5.6 mg GAE 100 g^{-1} of FW) and tamarind (83.8 ± 6.1 mg GAE 100 g^{-1} of FW), and lower than those found in acerola (861 ± 62 mg GAE 100 g^{-1} of FW), which has been widely commercialized as frozen pulp and juice (Hassimotto et al., 2005; Almeida et al., 2011).

The dilution step of the açaí pulp reduced total polyphenols to more than 70% compared to the initial concentration. The results of the polyphenol concentrations found in the permeate and retentate samples were compared with those of the feed suspensions.

Average reductions of total polyphenols were 43% (±5.9%) in the permeates and 7.3% (±7.2%) in the retentates. The reduction of total polyphenol contents in the retentate may be due to oxidation reactions occurring in the feed tank. Additional losses can be attributed to the action of the endogenous enzymes present in the pulp. Cruz et al. (2011) reported a 57.3% reduction of total phenolics (from 331.3 to 141.5 GAE 100 g^{-1} of FW) in the permeate fraction and a 28.5% increase of total phenolics (from 331.3 to 425.8 GAE 100 g^{-1} of FW) in the retentate fraction after microfiltration using 0.1 μm pore size alumina ceramic membranes. The authors also injected nitrogen gas into the system in order to minimize oxidation reactions. Pacheco-Palencia et al. (2007) found that the clarification process (vacuum filtering through filter paper, followed by passing through diatomaceous earth) caused a 27% drop in the concentration of polyphenols in clarified pulp, in comparison to unclarified juice.

Permeates obtained from the microfiltration of enzyme-treated pulp showed less reduction on average (40%) than those from untreated pulp (46%), indicating that enzyme treatment improved the permeation of polyphenols through all membranes used in the microfiltration experiments (Fig. 5). Using the *t*-test, the

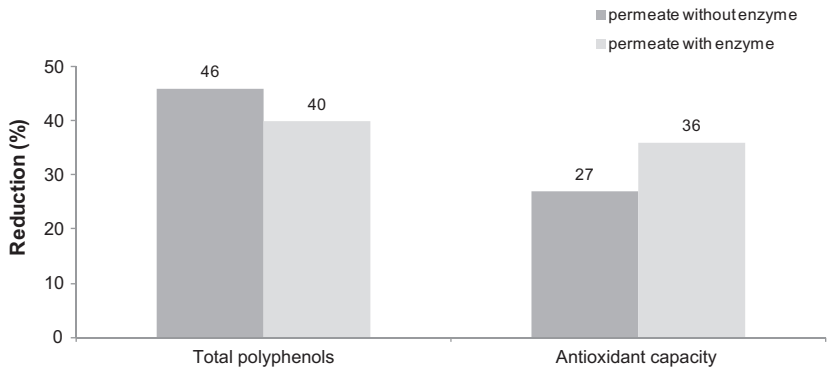

Fig. 5. Percentage reduction of total polyphenols content (mg GAE 100 mL^{-1}) and antioxidant capacity (μmol of TEAC 100 mL^{-1}) in the permeate in relation to the feed suspension (diluted açaí pulp with or without enzyme treatment).

percentages of reduced total polyphenols differed significantly ($p < 0.01$) between permeates obtained from enzyme-treated and untreated pulp.

Data in the literature indicate that the extraction of polyphenols from fruits such as grapes and blackcurrants could be due to the random release of these compounds from the skin cell wall in response to the progressive enzymatic degradation of cell wall polysaccharides. Furthermore, the use of enzymes could enhance the juice yield and the extraction of polyphenols, suggesting a positive linear correlation between the degradation of the polysaccharides and the amount of polyphenols released (Bagger-Jørgensen and Meyer, 2004; Koponen et al., 2008).

Table 5 shows the variation in antioxidant capacity in the açaí pulp, feed suspension, permeate and retentate samples.

The antioxidant capacity of a food is usually determined by a combination of methods due to the presence of different antioxidants with different action mechanisms. As the purpose of this study was to evaluate products originated by the cross-microfiltration process (permeate and retentate), when compared to feed suspension from the microfiltration experiments, only one method was used to determine the *in vitro* antioxidant capacity of the samples. The method chosen was the 2,2-diphenyl-1-picrylhydrazyl (DPPH·) radical scavenging assay, which is among the most popular spectrophotometer methods to determine the antioxidant capacity in foods and chemical compounds, due to the chemical stability of its free radical (Brand-Williams et al., 1995; Sanchez-Moreno, 2002; Molyneux, 2004).

The antioxidant capacity measured in the five brands of commercial açaí pulp ranged from 1436 to 1760 μmol of trolox equivalent antioxidant capacity (TEAC) per 100 mL of the sample. As discussed above for total polyphenols, it was also difficult to compare the antioxidant capacity values found in this study with those of other studies due to several factors, primarily the use of different determination methods.

As an example, Pozo-Insfran et al. (2004) and Pacheco-Palencia et al. (2007) determined the antioxidant capacity of açaí pulp using ORAC assay (oxygen radical absorbance capacity) and found 4860 μmol TEAC 100 mL^{-1} and 5440 ± 170 TEAC 100 mL^{-1}, respectively. Cruz et al. (2011) determined the antioxidant capacity using the ABTS [2,29-azinobis-(3-ethylbenzothiazoline-6-sulfonic acid] assay and found 2780 ± 100 μmol TEAC 100 g^{-1} of açaí pulp after maceration of the fruit. These findings represent relatively high antioxidant content in comparison with the values found in this study.

The antioxidant capacity found in açaí pulp (>1400 μmol TEAC 100 mL^{-1} of sample) was higher than those of other Brazilian exotic fruits with considerable market potential, such as murici (646 ± 31 mg TEAC 100 g^{-1} of FW), mangaba (527 ± 34 mg TEAC 100 g^{-1} of FW) and tamarind (204 ± 48 mg TEAC 100 g^{-1} of FW), which were determined using the DPPH· assay (Almeida et al., 2011). The dilution step for açaí pulp reduced the antioxidant capacity more than 79% from the initial value.

The average reduction of μmol TEAC per 100 mL of the permeate (31.6% ± 10.8%) obtained after microfiltration of enzyme-treated pulp was significantly higher ($p < 0.01$) than that obtained after microfiltration of untreated pulp (Fig. 5). As for polyphenols, the reduced antioxidant capacity of the retentate (25.5% ± 12.7%) was due to the oxidation and enzymatic reactions carried out in the feed tank during the microfiltrations. Similar results were found by other authors (Cruz et al., 2011; Pacheco-Palencia et al., 2007), which found reduced antioxidant capacity after açaí juice clarification.

As the antioxidant capacity efficiency of polyphenols greatly depends on their chemical structure (Bravo, 1998), one reason for decreased antioxidant capacity in the permeates for treated pulp can be associated with heating the pulp to 35 °C to induce enzyme activity. Although the 30 min-period for enzyme incubation is short, it may have been enough to affect the chemical structure

Table 5
Antioxidant capacity (μmol TEAC 100 mL^{-1}) of açaí pulp, feed suspension (untreated and enzyme-treated), and products (permeate and retentate) obtained after cross-flow microfiltrations.

Samples	Microfiltrations					
	MF1	MF2	MF3	MF4	MF5	MF6
Açaí pulp[a]	1653 ± 46.2	1695 ± 16.7	1760 ± 34.6	1547 ± 57.7	1606 ± 85.5	1436 ± 69.4
Feed	400 ± 0.0	365 ± 5.1	367 ± 10.1	294 ± 7.7	358 ± 10.2	230 ± 1.9
Permeate	335 ± 23.4 (16)[b]	258 ± 8.4 (29)	269 ± 15.1 (27)	154 ± 6.9 (48)	248 ± 1.9 (31)	140 ± 5.1 (39)
Retentate	353 ± 16.2 (12)	221 ± 7.7 (39)	317 ± 12.9 (14)	179 ± 1.9 (39)	246 ± 3.3 (31)	189 ± 1.9 (18)

TEAC: μmol of trolox equivalent antixodiant capacity per 100 mL of sample
Data are expressed as the mean of three replicates ± standard deviations
[a] açaí pulp *in natura* (untreated).
[b] Percentage reduction in comparison with the feed.

of the compounds responsible for antioxidant capacity, specifically the anthocyanins in which stability is adversely affected by temperature. Additionally, enzyme activity on the açaí pulp may have caused changes in the polyphenols profile affecting their ability to scavenge the DPPH· free radical (Buchert et al., 2005; Koponen et al., 2008).

4. Conclusion

The 0.2 μm pore size membrane performed better than its 0.8 μm counterpart. Moreover, the results showed a positive effect of pectin lyase on the cross-flow microfiltration process of açaí pulp, yielding the highest flux and lowest total membrane resistance, which can be attributed to enzyme action on the pectic compounds.

Cake filtration was the dominant mechanism in the early stages of most of the microfiltration processes. After approximately 20 min, however, intermediate pore blocking and complete pore blocking contributed to the overall fouling mechanisms.

In general, the mechanisms that cause fouling and the influence of membrane properties on such mechanisms are not yet understood. Dissolved substances such as proteins, polysaccharides and polyphenols are involved in the formation of fouling, but the individual impact on porous membrane blocking has not yet been determined. Further studies on fouling layer structural morphology using microscopy techniques will be undertaken.

Acknowledgements

The authors gratefully acknowledge the financial support and post-doctoral fellowship (R.M.D. Machado) from the São Paulo Research Foundation (FAPESP 2009/05938-1), as well as the valuable technical assistance provided by Silviane Zanni Hubinger (Brazilian Agricultural Research Corporation).

References

Almandoz, C., Pagliero, C., Ochoa, A., Marchese, J., 2010. Corn syrup clarification by microfiltration with ceramic membranes. J. Membr. Sci. 363, 87–95.

Almeida, M.M.B., Sousa, P.H.M., Arriaga, A.M.C., Prado, G.M., Magalhães, C.E.C., Maia, G.A., Lemos, T.L.G., 2011. Bioactive compounds and antioxidant activity of fresh exotic fruits from northeastern Brazil. Food Res. Int. 44, 2155–2159.

Araújo, M.C.P., Gouvêa, A.C.M.S., Couto, D.S., Cabral, L.M.C., Godoy, R.L.O., Freitas, S.P., 2011. Effect of enzymatic treatment on the viscosity of raw juice and anthocyanins content in the microfiltrated blackberry juice. Desalination Water Treat. 27, 37–41.

Arnot, T.C., Field, R.W., Koltuniewicz, A.B., 2000. Cross-flow and dead-end microfiltration of oily-water emulsions. Part II. Mechanisms and modelling of flux decline. J. Membr. Sci. 169, 1–15.

Astudillo, C., Parra, J., González, S., Cancino, B., 2010. A new parameter for membrane cleaning evaluation. Sep. Purif. Technol. 73, 286–290.

Bagger-Jørgensen, R., Meyer, A.S., 2004. Effects of different enzymatic pre-press maceration treatments on the release of phenols into blackcurrant juice. Eur. Food Res. Technol. 219, 620–629.

Belfort, G., Davis, R.H., Zydney, A.L., 1994. Review: the behavior of suspensions and macromolecular solutions in cross-flow microfiltration. J. Membr. Sci. 96, 1–58.

Benen, J.A.E., Voragen, A.G.J., Visser, J., 2003. Pectic enzymes. In: Whitaker, J.R., Voragen, A.G.J., Wong, D.W.S. (Eds.), Handbook of Food Enzymology. Marcel Dekker, Inc., New York, p. 1079.

Borovik, C.P.B., 2010. Fracionamento de Polpa de Açaí e Concentração de Antocianinas utilizando Membranas Poliméricas. Dissertação (Mestrado em Engenharia de Alimentos) – Faculdade de Engenharia de Alimentos. Universidade Estadual de Campinas, Campinas-SP, p. 89.

Brand-Williams, W., Cuvelier, M.E., Berset, C., 1995. Use of a free radical method to evaluate antioxidant activity. Lebensm. Wiss. Technol. 28, 25–30.

Bravo, L., 1998. Polyphenols: chemistry, dietary sources, metabolism, and nutritional significance. Nutr. Rev. 56, 317–333.

Buchert, J., Koponen, J.M., Suutarinen, M., Mustranta, A., Lille, M., Törrönen, R., Poutanen, K., 2005. Effect of enzyme-aided pressing on anthocyanin yield and profiles in bilberry and blackcurrant juices. J. Sci. Food Agr. 85, 2548–2556.

Castañeda-Ovando, A., Pacheco-Hernández, M.L., Páez-Hernández, M.E., Rodríguez, J.Á., Galán-Vidal, C.A., 2009. Chemical studies of anthocyanins: a review. Food Chem. 113, 859–871.

Cheryan, M., 1998. Ultrafiltration and Microfiltration Handbook. Technomic Publishing Company, Lancaster, p. 527.

Cruz, A.P.G., Mattietto, R.A., Taxi, C.M.A.D., Cabral, L.M.C., Donangelo, C.M., Matta, V.M., 2011. Effect of microfiltration on bioactive components and antioxidant activity of açaí (*Euterpe oleracea* Mart.). Desalination Water Treat. 27, 97–102.

Dufrèche, J., Prat, M., Schmitz, P., 2002. Effective hydraulic resistance of the first cake layers at the membrane surface in microfiltration. Desalination 145, 129–131.

Field, R.W., Wu, D., Howell, J.A., Gupta, B.B., 1995. Critical flux concept for microfiltration fouling. J. Membr. Sci. 100, 259–272.

Gan, Q., Howell, J.A., Field, R.W., England, R., Bird, M.R., McKechinie, M.T., 1999. Synergetic cleaning procedure for a ceramic membrane fouled by beer microfiltration. J. Membr. Sci. 155, 277–289.

George, S., Brat, P., Alter, P., Amiot, M.J., 2005. Rapid determination of polyphenols and vitamin C in plant-derived products. J. Agric. Food Chem. 53, 1370–1373.

Hassimotto, N.M.A., Genovese, M.I., Lajolo, F.M., 2005. Antioxidant activity of dietary fruits, vegetables, and commercial frozen fruit pulps. J. Agric. Food Chem. 53, 2928–2935.

Hermia, J., 1982. Constant pressure blocking filtration laws – application to power-law non-newtonian fluids. Trans. IChem. E. 60, 183–187.

Hu, B., Scott, K., 2008. Microfiltration of water in oil emulsions and evaluation of fouling mechanism. Chem. Eng. J. 136, 210–220.

Kashyap, D.R., Vohra, P.K., Chopra, S., Tewari, R., 2001. Applications of pectinases in the commercial sector: a review. Bioresour. Technol. 77, 215–227.

Koponen, J.M., Buchert, J., Poutanen, K.S., Törrönen, A.R., 2008. Effect of pectinolytic juice production on the extractability and fate of bilberry and black currant anthocyanins. Eur. Food Res. Technol. 227, 485–494.

Kris-Etherton, P.M., Hecker, K.D., Bonanome, A., Coval, S.M., Binkoski, A.E., Hilpert, K.F., Griel, A.E., Etherton, T.D., 2002. Bioactive compounds in foods: their role in the prevention of cardiovascular disease and cancer. Am. J. Med. 113, 71S–88S.

Li, M., Zhao, Y., Zhou, S., Xing, W., 2010. Clarification of raw rice wine by ceramic microfiltration membranes and membrane fouling analysis. Desalination 256, 166–173.

Lichtenthäler, R., Belandrino, R., Maia, J., Papagiannopoulos, M., Fabricius, H., Marx, F., 2005. Total antioxidant scavenging capacities of *Euterpe oleracea* Mart. (açaí) fruits. Int. J. Food Sci. Nutr. 56, 53–64.

Lim, A.L., Bai, R., 2003. Membrane fouling and cleaning in microfiltration of activated sludge wastewater. J. Membr. Sci. 216, 279–290.

Menezes, S.E.M., Torres, A.T., Srur, A.U.S., 2008. Valor nutricional da polpa de açaí (*Euterpe oleracea* Mart.) liofilizada. Acta Amazônica 38, 311–316.

Miller, J.C., Miller, J.N., 1993. Statistics for analytical chemistry. Ellis Horwood PTR Prentice-Hall, New York, 3rd ed., p. 233.

Mirsaeedghazi, H., Emam-Djomeh, Z., Mousavi, S.M., Aroujalian, A., Navidbakhsh, M., 2010. Clarification of pomegranate juice by microfiltration with PVDF membranes. Desalination 264, 243–248.

Molyneux, P., 2004. The use of the stable radical diphenylpicryl-hydrazyl (DPPH) for estimating antioxidant activity. Songklanakarin J. Sci. Technol. 26, 211–219.

Pacheco-Palencia, L.A., Hawken, P., Talcott, S.T., 2007. Phytochemical, antioxidant and pigment stability of açaí (*Euterpe oleracea* Mart.) as affected by clarification, ascorbic acid fortification and storage. Food Res. Int. 40, 620–628.

Pilnik, W., Voragen, A.G.J., 1993. Pectic enzymes in fruit and vegetable juice manufacture. In: Nagodawithama, T., Reed, G. (Eds.), Enzymes in Food Processing, 3rd ed. Academic Press Inc., London, p. 480.

Pozo-Insfran, D., Brenes, C.H., Talcott, S.T., 2004. Phytochemical composition and pigment stability of açaí (*Euterpe oleracea* Mart.). J. Agric. Food Chem. 52, 1539–1545.

Rai, C., Rai, P., Majumdar, G.C., De, S., DasGupta, S., 2010. Mechanism of permeate flux decline during microfiltration of watermelon (*Citrullus lanatus*) juice. Food Bioprocess Technol. 3, 545–553.

Rogez, H., 2000. Açaí: preparo, composição e melhoramento da conservação. Ed. Universidade Federal do Pará – EDUPA, Belém, Pará, p. 300.

Rufino, M.S.M., Pérez-Jiménez, J., Arranz, S., Alves, R.E., Brito, E.S., Oliveira, M.S.P., Saura-Calixto, F., 2011. Açaí (*Euterpe oleraceae*) 'BRS Pará': a tropical fruit source of antioxidant dietary fiber and high antioxidant capacity oil. Food Res. Int. 44, 2100–2106.

Sanchez-Moreno, C., 2002. Review: methods used to evaluate the free radical scavenging activity in foods and biological systems. Food Sci. Technol. Int. 8, 121–137.

Schauss, A.G., Wu, X., Prior, R.L., Ou, B., Patel, D., Huang, D., Kababick, J.P., 2006. Phytochemical and nutrient composition of the freeze-dried Amazonian palm berry, *Euterpe oleraceae* Mart. (Acai). J. Agric. Food Chem. 54, 8598–8603.

Singleton, V.L., Rossi, J.A., 1965. Colorimetry of total phenolics with phosphomolybdic–phosphotungstic acid reagents. Am. J. Enol. Viticult. 16, 144–158.

Song, L.F., Elimelech, M., 1995. Theory of concentration polarization in crossflow filtration. J. Chem. Soc. Faraday Trans. 91, 3389–3398.

Szajdek, A., Borowska, E.J., 2008. Bioactive compounds and health-promoting properties of berry fruits: a review. Plant Foods Hum. Nutr. 63, 147–156.

Trevisan, B.P., 2011. Avaliação da tensão superficial, parâmetros reológicos e atenuação acústica de suspensões de açaí. São Carlos, Dissertação (Mestrado em Engenharia Mecânica) – Escola de Engenharia de São Carlos. Universidade de São Paulo, São Carlos-SP, p. 114.

Ushikubo, F.Y., Watanabe, A.P., Viotto, L.A., 2007. Microfiltration of umbu (*Spondias tuberosa* Arr. Cam.) juice. J. Membr. Sci. 288, 61–66.

Vaillant, F., Millan, P., O'Brien, G., Dornier, M., Decloux, M., Reynes, M., 1999. Crossfow microfltration of passion fruit juice after partial enzymatic liquefaction. J. Food Eng. 42, 215–224.
Yadav, S., Yadav, P.K., Yadav, D., Yadav, K.D.S., 2009. Pectin lyase: a review. Process Biochem. 44, 1–10.
Yu, J., Lencki, R.W., 2004. Effect of enzyme treatments on the fouling behavior of apple juice during microfiltration. J. Food Eng. 63, 413–423.
Zeman, L.J., Zydney, A.L., 1996. Microfiltration and Ultrafiltration: Principles and Applications. Marcel Dekker, New York, p. 618.